Enhanced mapping of a smallholder crop farming landscape through image fusion and model stacking

Wonga Masiza[a ,b,*] , Johannes George Chirima[b ,c] , Hamisai Hamandawana[a] , and Rajendran Pillay[a]

[a] Department of Geography and Environmental Science, University of Fort Hare, Alice, South Africa
[b] Geoinformation Science Division, Agricultural Research Council-Institute for Soil, Climate and Water, Pretoria, South Africa
[c] Centre for Geoinformation Science, Department of Geography, Geoinformatics and Meteorology, University of Pretoria, Pretoria, South Africa

*Contact: Wonga Masiza. Department of Geography and Environmental Science, University of Fort Hare, Alice 5700, South Africa. Email: iconMasizaW@arc.agric.za

Abstract

Globally, Smallholder farming systems (SFS) are recognized as one of the most important pillars of rural economic development and poverty alleviation because of their contribution to food security. However, support for this agricultural sector is hampered by lack of reliable information on the distributions and acreage of smallholder fields. This information is essential in not only monitoring food security and informing markets but also in guiding the determination of levels of support required from government by individual farmers. There is urgent need for robust techniques that can be used to cost-effectively and time-efficiently map smallholder crop fields especially in Sub-Saharan Africa and Asia. This study attempts to do this by using an approach in which optical and Synthetic Aperture Radar (SAR) data are systematically combined and classified using Extreme Gradient Boosting (Xgboost). We also investigated model stacking as another technique to improve classification accuracy. We combined Xgboost with Random Forest (RF), Support Vector Machine (SVM), Artificial Neural Networks (ANN), and Naïve Bayes (NB). The combined use of multi-temporal Sentinel-2 bands, spectral indices, and Sentinel-1 produced better results than exclusive use of optical data (α = 0.95, p = 0.0005). Furthermore, stacking of classification algorithms based on model comparisons achieved higher accuracy than stacking the algorithms indiscriminately (α = 0.95, p = 0.0100). Through systematic fusion of SAR and optical data and hyper-parameter tuning of Xgboost, we achieved a maximum classification accuracy of 97.71%, while achieving a maximum accuracy of 96.06% through model stacking. This highlights the importance of multi-sensor data fusion and multi-classifier systems when mapping fragmented agricultural landscapes.

1. Introduction

Smallholder farming systems (SFS) dominate the 570 million farms around the world (Graeub et al. 2016; Lowder, Skoet, and Raney 2016; Samberg et al. 2016), and are increasingly seen as a pivotal niche for economic development and food security (Aliber and Hart 2009; Rapsomanikis 2015; UNCTAD 2015). However, the farmers' capacity to enhance realization of this objective is undermined by numerous constraints. These include extreme weather events (Chapagain and Raizada 2017; Harvey et al. 2018; Manderson, Kubayi, and Drimie 2016; Mugambiwa and Tirivangasi 2017), ineffective response to shocks (Devereux 2007), infrastructural bottlenecks and limited capital (ASFG, 2013; Khapayi and Celliers 2016; Von Fintel and Pienaar 2016), poor extension services (Akpalu 2013; Fanadzo and Ncube 2018), inappropriate land tenure arrangements (Bembridge 2000), and lack of good quality data among many (Carletto, Jolliffe, and Banerjee 2013; Lowder, Skoet, and Raney 2016; Samberg et al. 2016). Data quality is very crucial because of the role of data in science, while NGOs, governments, creditors, policymakers, and insurers rely on agricultural statistics in allocating resources and providing services to farmers (Carletto, Jolliffe, and Banerjee 2013; Samberg et al. 2016). The most basic data required from crop production systems are spatial data, which include the amount of area under cultivation and the distribution of crop fields.

Methods that have been used to locate and measure cropped areas include; soliciting information from farmers (FAO 2016), use of Global Positioning Systems (GPS) (Keita, Carfagna, and Mu'Ammar 2010), digitization of high-resolution satellite and aerial images (FAO 2016), pixel-based and object-based image classification (Dhumal et al. 2013). Amongst these, image classification is regarded as the most time-efficient, cost-effective, and objective technique. However, there are still unresolved complications using this method because of the difficulties involved in the spectral discrimination of

different crops and other vegetation types (Rao 2008), landscape heterogeneity in smallholder farming areas (Debats et al. 2016), irregular shapes and sizes of SFS (Persello et al. 2019) and the inter-annual fluctuation of cultivated land (Nieuwoudt and Groenewald 2003). To address these challenges, researchers are riding the wave of 'big data' and machine learning exploring ways in which multi-sensor and multi-temporal data can assist in producing reliable crop maps. Multi-temporal imagery improves accuracy in discriminating crops and other vegetation types because of its ability to model phenological differences between plants (Aguilar et al. 2018; Brisco, Ulaby, and Protz 1984; Debats et al. 2016; Useya and Chen 2019; Zurita-Milla, Izquierdo-Verdiguier, and De By 2017). Use of multi-sensor data produces improved results (Dimov et al. 2017; Forkuor et al. 2014; Van Tricht et al. 2018; Zhou et al. 2017) while Synthetic Aperture Radar (SAR), unlike optical data, is not limited by atmospheric conditions.

The challenge in mapping SFS is not only in requiring optimum combinations of datasets but it is also in the optimization of mapping algorithms. While most research has been comparing different machine learning classifiers, there is also a growing interest in multi-classifier systems. The practice of combining classification algorithms is predicated on the hypothesis that integrating multiple classifiers produces a more powerful model. To the best of our knowledge, still very few studies have tested this approach in mapping SFS. Furthermore, Wu, Wang, and Wu (2012) noted that model stacking, in particular, is less popular in remote sensing applications. A few notable studies that used this approach include Aguilar et al. (2018)'s combination of Random Forest (RF), Maximum Entropy, and Support Vector Machines (SVM). Sonobe et al. (2018) combined SVM and RF for crop classification in Japan. Useya and Chen (2018) mapped SFS in Zimbabwe by combining Maximum Likelihood Classification, SVM, and Spectral Information Divergence. Salas et al. (2019) combined Generalized Linear Model, RF, Boosted Regression Trees, Maximum Entropy, and Multivariate Adaptive Regression Splines to map crop types in a highly fragmented landscape in India. All these studies reported that combining the models improved classification accuracy compared to using a single classifier. However, we observed that the authors combined the algorithms indiscriminately.

In this study, we compare the effectiveness of image fusion and model stacking in improving mapping accuracy of a smallholder farming landscape. We take a slightly different approach in our classification experiments. From a stack of 40 multi-temporal Sentinel-2 bands, we filter out unimportant images using a variable importance algorithm. We then compute different optical indices, which are selected based on their sensitivities to different surface features. We combine these with the vertical transmit, horizontal receive (VH) and vertical transmit, vertical receive (VV) polarimetric bands of Sentinel-1 in a series of classification trials, searching for an optimum combination of these datasets. We use the Extreme Gradient Boosting (Xgboost) classifier partly because it is recently developed, and has been outperforming other algorithms in machine learning competitions (Nielsen 2016). To perform model stacking, we combine Xgboost with RF, SVM, Artificial Neural Networks (ANN), and Naïve Bayes (NB). We first stack all the classifiers indiscriminately, and then compare this with stacking that is based on model comparisons. This is informed by the idea that model stacking should be an ensemble of sub-models that are weakly correlated (Džeroski and Ženko 2004; Merz 1999). Essentially, the study is a search for optimum results through fusion of SAR and optical data, and through model stacking.

2. Materials and methods

2.1. Study area

The O.R. Tambo District Municipality (ORTDM) is in the Eastern Cape Province of South Africa (Figure 1).
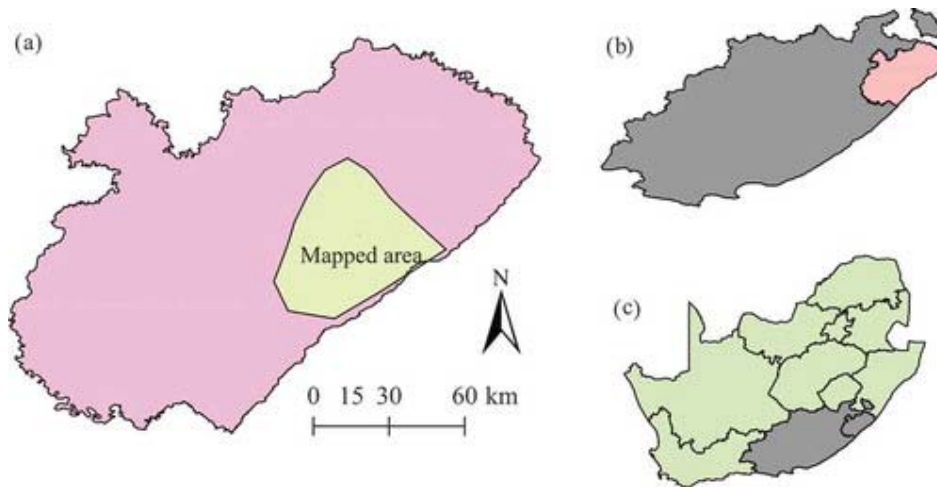
Figure 1. Location of (*a*) ORTDM in (*b*) Eastern Cape Province, (*c*) South Africa.

The district is part of the former Transkei homelands and the majority (94%) of its 1 364 943 population (2011 Census) live in villages. The major sources of livelihood include social grants from government, livestock farming, and crop production in the form of maize, tea, cannabis, and vegetables (ECSECC 2014; Municipality 2017). Agriculture is practised in an environment in which mean annual rainfall ranges between 900 mm and 1300 mm, with summer minimum and maximum temperatures that range between 14°C and 19°C and 14°C and 27°C, respectively (Jordaan et al. 2017). Majority of the smallholder farms produce only maize, partly because they get inputs from the government, and because of the mielie-meal producing RED Hub project, which has a significant impact on rural income (Iortyom, Mazinyo, and Nel 2018). The crop fields range from a minimum of backyard – one hectare plots to bigger collective farms in which a number of individual smallholders own plots. Crop production intensifies during the wet season (October to April) with planting dates ranging between November and January depending on the commencement of the rainfall season. Although most of the farmers sell their produce to local supermarkets, animal feed retailers, and milling plants, part of this is usually destined for domestic consumption (DRDLR 2016)

2.2. Image compilation and pre-processing

The materials used comprise multi-date Sentinel-2 Level-1C and Sentinel-1 Level-1 Ground Range Detected (GRD) images. Table 1 provides the identity details, which include acquisition dates and percentages of cloud cover in the images, used to compile footprint coverages of the study area.

Table 1. List of images providing footprint coverages of the study area.

Sensor	Image ID	
Sentinel – 2	L1C_T35HPE_A013245_20180104T080546	L1C_T35JPF_A013245_20180104T080546
	L1C_T35JPF_A005123_20180228T075917	L1C_T35HPE_A013717_20180206T081553
	L1C_T35HPE_A014432_20180328T081650	L1C_T35JPF_A014432_20180328T081650
	L1 C_T35HPE_A005881_20180422T081053	L1 C_T35JPF_A005881_20180422T081053
Sentinel-1	S1A_IW_GRDH_1SDV_20180113T164515_20180113T164540_020138_022584_6743	
	S1A_IW_GRDH_1SDV_20180218T164515_20180218T164540_020663_02363B_4B89	
	S1A_IW_GRDH_1SDV_20180326T164515_20180326T164540_021188_0246E4_A133	
	S1A IW GRDH 1SDV 20180419T164516 20180419T164541 021538 0251D4 89FD	

All the Sentinel 2 images were cloud-free

Sentinel-2 images consisted of four pairs of tiles, each of which provided a representative footprint coverage of crop-producing areas in the ORTDM. We purposely excluded the low-resolution bands of Sentinel-2 and proceeded to use the 20 m and 10 m resolution bands. Sentinel-2 images were pre-

processed by using the Sen2Cor 2.5.5 plugin tool to correct Top-Of-Atmosphere (TOA) Level-1C reflectance to Bottom-Of-Atmosphere (BOA) surface reflectance. Thereafter, individual pairs of Sentinel-2 images were mosaicked in QGIS. Each of the four Sentinel-1 images were big enough to cover the study area and were acquired in the conflict-free VV and VH polarizations, with a 250 km Interferometric Wide (IW) swath mode, at 5 m by 20 m spatial resolution, projected to WGS84. Pre-processing techniques applied on Sentinel-1 imagery included: 1) Orbit file application, 2) Radiometric calibration, 3) Speckle filtering, and 4) Geometric correction. Afterwards, both the Sentinel-1 and Sentinel-2 bands were co-registered to WGS84 UTM Zone 35 S and resampled to 10 m resolution.

2.3. Field work

Field data were collected between May and July 2018 with the location of crop fields being aided by a field guide map that was prepared from crop cultivation records of 2017 to 2018 season acquired from extension officers of the Department of Rural Development and Agrarian Reform (DRDAR). These records include geocoded lists of crop fields with contact details of all smallholder farmers who had planted maize, cannabis, and vegetables in the 2017 to 2018 season. Since there were very few legal cannabis farms at the time, we accessed the remote illegal farms with the assistance of farmers. While we visited most of the maize and vegetable farms, we confirmed the DRDAR-solicited information through telephone interviews for the few we could not visit. The tea farms are well known and easily identified on Sentinel-2 images and Google Earth. We recorded GPS coordinates of each crop field, which we then edited in Google Earth and ArcGIS to generate training polygons. We also collected GPS coordinates of other land use and land cover types in order to enhance confident discrimination of crop fields. Table 2 summarizes the information classes for which detailed information was compiled.

Table 2. Information classes identified during field investigation.

Class code	Name	Description
1	Maize	Maize-cultivated crop fields
2	Vegetables	Intercropping of cabbage, beetroot, and spinach
3	Cannabis	Cannabis crop fields
4	Tea	Magwa and Majola Tea Estates
5	Planted forest	Forest plantations
6	Grassland	Open grassland with < 10% trees and canopy cover
7	Urban	Villages, buildings, and other man-made structures
8	Bare soil	Non-vegetated areas with bare soil and rock outcrops
9	Clear water	Surface water bodies with clear water
10	Dense natural trees	Densely distributed trees ≥ 2 m tall
11	Sparse natural trees	Sparsely distributed trees ≥ 2 m tall
12	Turbid water	Surface water bodies with suspended sediment
13	Shrub	Herbaceous plants ≤ 1 m tall

2.4. Image analysis

The procedures applied for image analysis include 1) systematic compilation of predictor variables from the satellite images, 2) fusion of Sentinel-1 and Sentinel-2 in a systematically determined number of classification trials, and 3) classification through model stacking.

2.4.1. Compilation of predictor variables and image classification

We applied variable importance (VI) to rank 40 multitemporal Sentinel-2 bands. We used the Mean Decrease Accuracy (MDA), which is a variable ranking measure of RF to rank the explanatory power of each band. The MDA is computed as shown in Equation 1 by calculating and averaging predictor errors in out-of-bag (OOB) data before and after permutation (Hur, Ihm, and Park 2017; Souri and Vajedian 2015).

$$\mathrm{VI}^t_{(x_j)} = \frac{\sum_{i \in (\mathrm{OOB})^t} \mathrm{I}(y_i = f(x_i))}{\left|(\mathrm{OOB})^t\right|} - \frac{\sum_{i \in (\mathrm{OOB})^t} \mathrm{I}\left(y_i = f\left(x_i^j\right)\right)}{\left|(\mathrm{OOB})^t\right|}$$

(1)

where

x_j is variable j in tree t,

$y_i = f(x_i)$ is the predicted class for observation i before permuting x_j, and;

$y_i = f\left(x_i^j\right)$ is predicted class for observation i after permuting variable x_j.

$(\mathrm{OOB})^t$ is the out of bag sample for a tree t.

This technique improves prediction by aiding the identification and elimination of redundant variables. The top 10 Sentinel-2 bands ranked as the most important were then used in further analyses. We selected four spectral indices because of their different sensitivities to different surface features. The Soil Adjusted Vegetation Index (SAVI) was computed using the Sentinel-2 image of January. SAVI minimizes the effects of soil reflectance on vegetation and is sensitive to leaf area index in the early stages of crop growth (Hatfield and Prueger 2010). SAVI is calculated according to Equation (2).

$$\mathrm{SAVI} = \frac{(\mathrm{NIR}) - (\mathrm{RED})}{(\mathrm{NIR}) + (\mathrm{RED}) + L \times (1 + L)}$$

(2)

RED and NIR are the red and near infrared wavelengths, respectively, while L is the canopy background (soil) adjustment factor. We computed Normalized Difference Vegetation Index (NDVI) using the Sentinel-2 image of February. NDVI performs best when vegetation density is low (Phadikar

and Goswami 2016; Xue and Su 2017) and is calculated according to Equation (3).

$$\mathrm{NDVI} = \frac{(\mathrm{NIR}) - (\mathrm{RED})}{(\mathrm{NIR}) + (\mathrm{RED})}$$

(3)

We computed the Two Band Enhanced Vegetation Index (EVI$_2$) for March and April. EVI$_2$ is more effective than NDVI when vegetation density is high and is less affected by canopy background signal and atmospheric influences (Jiang et al. 2008). It is calculated according to Equation (4).

$$\mathrm{EVI}_2 = 2.4 \frac{(\mathrm{NIR}) - (\mathrm{RED})}{(\mathrm{NIR}) + (\mathrm{RED}) + 1}$$

(4)

We computed the Normalized Difference Built-up Index (NDBI) using the Sentinel-2 image for March. NDBI includes the Short Wave Infrared (SWIR) band because urban surfaces have high reflectance in SWIR than other wavebands (Zha, Gao, and Ni 2003), and is calculated according to Equation (5).

$$\mathrm{NDBI} = \frac{(\mathrm{SWIR}) - (\mathrm{NIR})}{(\mathrm{SWIR}) + (\mathrm{NIR})}$$

(5)

We included NDBI because in ORTDM, crops are cultivated in immediate vicinities of urban features. From Sentinel-1, we used the VH and VV polarimetric bands. We selected these variables in order to facilitate the identification of combinations potentially capable of improving mapping accuracy when used with optical data. We used these variables in different combinations as inputs for different classification trials (Table 3).

Table 3. Data combinations as used in six different classification trials.

Trial	Input variable	Period	Total
1	S2 bands	January – April	10
2	S2 indices	January – April	*5
3	S2 bands, S2 indices	January – April	15
4	S2 bands, S2 indices, VH	January – April	19
5	S2 bands, S2 indices, VV	January – April	19
6	S2 bands, S2 indices, VH, VV	January – April	23

S1 = Sentinel-1, S2 = Sentinel-2, * EVI_2 was computed for March and April

2.4.2. Classification

Xgboost is an implementation of gradient boosting, which uses an additional regularization term in the objective function (Chen and Guestrin 2016). As in other ensemble tree-boosting algorithms, models are added in a sequential manner with the next predictor correcting errors made by previous predictors (weaker learners) until the training data are accurately predicted and no further improvements are made. This iterative process uses a gradient descent algorithm to optimize the loss function when adding new models by minimizing loss. The regularization term helps to avoid overfitting by controlling the complexity of the model. Using the caret package in R-Studio, we fine-tuned seven Xgboost hyper-parameters to optimize the models.

2.4.3. Model stacking

Model stacking is an ensemble technique that takes predictions generated by multiple machine learning algorithms and uses them as inputs in a second level learning classifier (Wolpert 1992). We used this technique to stack Xgboost, RF (Breiman 2001), SVM (Cortez and Vapnik 1995), ANN (Ripley 1996), and NB (Solares and Sanz 2007). We used the caret package to compute correlation coefficients (r) between the classifiers, after which we compared stacking of all the algorithms against stacking only weakly correlated models (Džeroski and Ženko 2004; Merz 1999).

2.4.4. Training and performance evaluation

We split the field-collected data into three chunks of independent datasets. Firstly, we split the data into 70% model building data, and 30% for model evaluation. Following (Géron 2019), we further split the model-building chunk into two subsets; the first subset to train the individual classifiers, and the second subset to generate new predictions, which we used as level two training data for model stacking. All the models were evaluated using the validation set. We evaluated the performance of the models by computing four model performance metrics, namely overall accuracy, Kappa coefficient (K), and model sensitivity and specificity (Rwanga and Ndambuki 2017). We then computed statistical significance tests to evaluate if the differences made by data fusion and model stacking were chance events or real improvements. We performed the tests at 0.95 confidence level using a model comparison R-function developed from the works of (Hothorn et al. 2005) and (Eugster, Hothorn, and Leisch 2008).

3. Results

The results of this investigation are presented under three sub-sections: sub-section 3.1 presents importance rankings of the Sentinel-2 bands, sub-section 3.2 summarizes results of data fusion, and sub-section 3.3 summarizes results of model stacking.

3.1. Variable rankings of the optical data

To reduce data redundancy and noise, we subjected the Sentinel-2 images to VI analysis and thereafter selected the top 10 multi-date image bands. Figure 2 shows ranks of the top 10 out of the 40 Sentinel-2 bands.
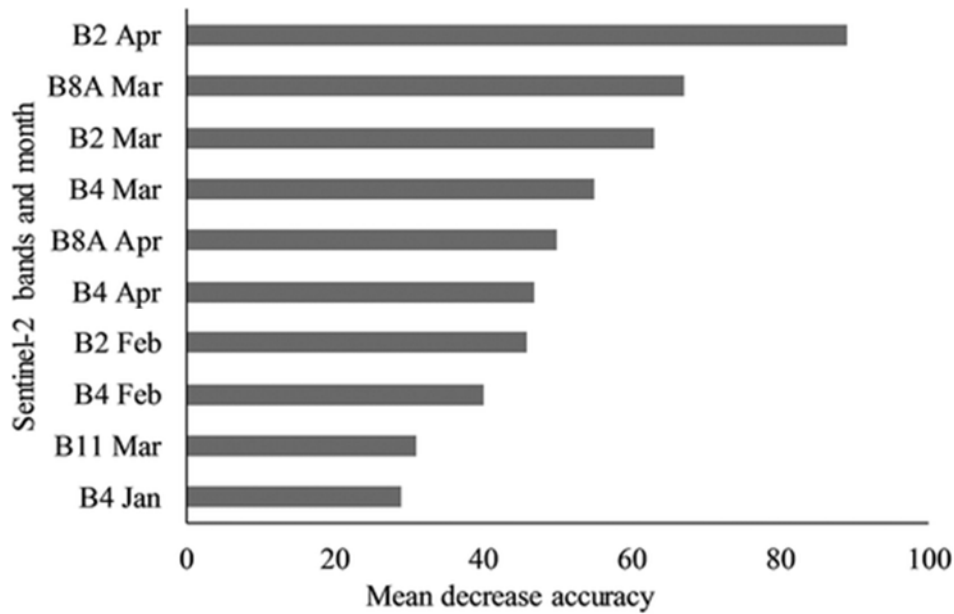
Figure 2. Top 10 of the 40 Sentinel-2 bands.

The top 10 bands out of the 40 include four images from March, three from April, two from February, and one from January, with bands B2, B8A, B4 and B11 being the most important variables.

3.2. Results of image fusion

Table 4 shows overall accuracies (OA), per-class Sensitivity (SE) and Specificity (SP), and Kappa coefficients (K) that we obtained by using Sentinel-2 data in the first three trials.

Table 4. Results of Sentinel-2 classification trials.

Class	Trial 1		Trial 2		Trial 3	
	SE	SP	SE	SP	SE	SP
Maize	100.00	99.98	100.00	99.93	100.00	99.98
Vegetables	4.55	100.00	18.18	100.00	9.09	100.00
Cannabis	44.44	100.00	16.67	99.99	22.22	100.00
Tea	99.76	99.84	96.48	97.02	99.76	99.80
Planted forest	90.53	99.90	87.96	99.80	90.20	99.90
Grassland	88.90	98.48	91.11	96.40	87.91	98.63
Urban	96.36	90.15	91.14	91.26	96.86	88.82
Bare soil	43.86	99.96	11.07	99.96	42.11	99.98
Clear water	95.00	100.00	95.00	99.96	95.00	100.00
Dense natural trees	85.92	99.92	78.40	99.71	88.03	99.90
Sparse natural trees	90.78	99.59	31.36	99.10	86.96	99.64
Turbid water	100.00	100.00	100.00	100.00	100.00	100.00
Shrubs	12.10	99.60	0.00	99.97	8.87	99.94
OA (%)	89.85		89.82		89.09	
K	77.40		76.55		75.95	

The results in Table 4 can be briefly summarized as follows:

We achieved the highest OA of Sentinel-2 through the exclusive use of the 10 multitemporal wavebands (89.85%) in trial 1. However, the spectral indices in trial 2 exhibited a superior sensitivity

to vegetables (18.18%) compared to the wavebands in trial 1 (4.55%) and the combination thereof (9.09%) in trial 3. The wavebands in trial 1 exhibited a superior sensitivity to cannabis (44.44%) than the spectral indices (16.67%) in trial 2 and the combination thereof (22.22%) in trial 3. The spectral indices exhibited less sensitivity (96.48%) to tea than the wavebands (99.76%) and the combination thereof (99.76%). Sensitivity to maize remained at 100% in all the Sentinel-2 trials. Figure 3 shows the classification maps we obtained from Sentinel-2 data.
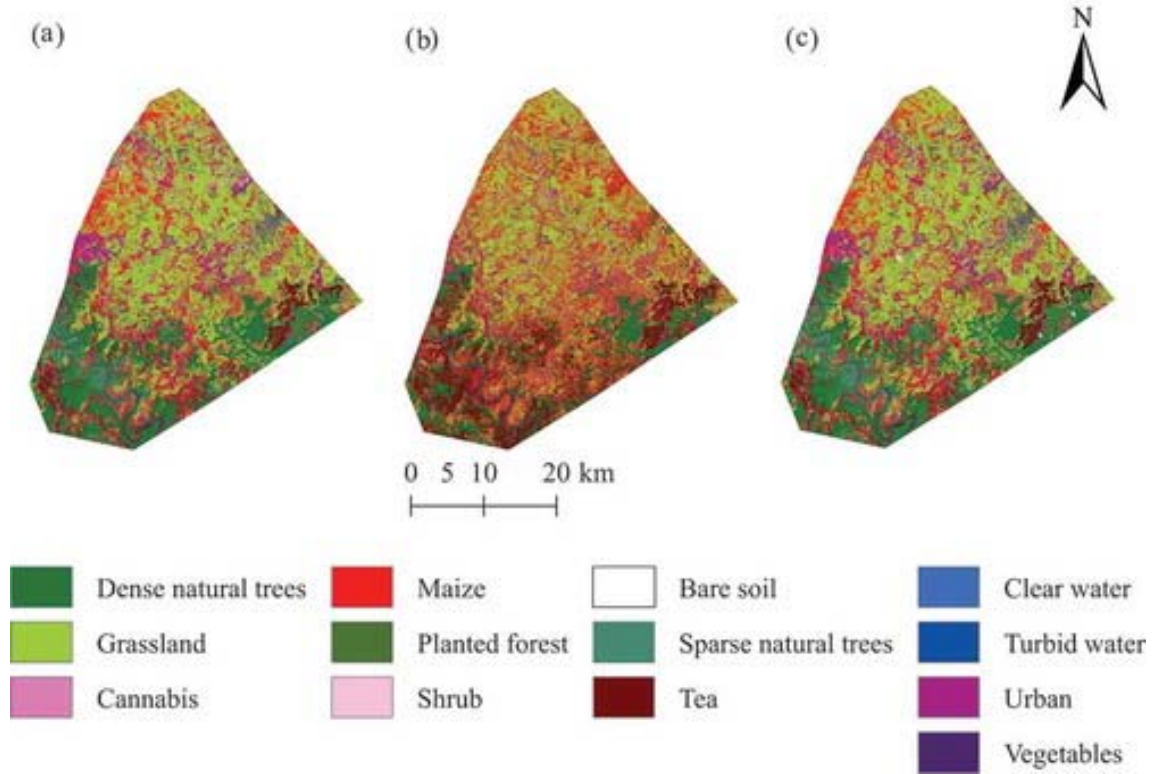

Figure 3. Classification of ORTDM with Sentinel-2 data: (*a*) Trial 1, (*b*) Trial 2, (*c*) Trial 3.

Table 5 presents the results we obtained by fusing optical and SAR datasets in trials 4 to 6.

Table 5. Results of fusing Sentinel-1 and Sentinel-2 data.

Class	Trial 4		Trial 5		Trial 6	
	SE	SP	SE	SP	SE	SP
Maize	100.00	99.99	100.00	99.98	100.00	99.99
Vegetables	0.00	100.00	13.64	100.00	0.00	100.00
Cannabis	33.33	100.00	22.22	99.97	11.11	99.84
Tea	99.88	99.80	99.84	99.90	99.98	99.88
Planted forest	90.03	99.90	90.03	99.88	90.12	100.00
Grassland	98.15	99.24	93.45	99.17	98.28	99.33
Urban	97.87	98.27	97.99	93.62	97.98	98.38
Bare soil	85.20	99.91	44.52	99.97	85.31	99.90
Clear water	95.00	100.00	95.00	100.00	95.00	100.00
Dense natural trees	89.44	99.88	86.15	99.90	88.26	99.89
Sparse natural trees	85.24	99.67	84.98	99.65	87.74	99.66
Turbid water	100.00	100.00	100.00	100.00	100.00	100.00
Shrubs	7.26	99.94	8.87	99.94	7.26	99.96
OA (%)	97.58		93.46		97.71	
K	94.00		84.67		94.33	

Highest OA with S2 = 89.85%, Highest OA with S1-S2 fusion = 97.71%

Difference = 7.86%, *p* = 0.0005

Combining optical data with both the VV and VH bands of SAR in trial 6 attained the highest OA (97.71%) compared to all the different combinations of SAR and optical data. Sensitivity to maize remained the same in all the trials (100%). Exclusive use of optical data in trial 2 exhibited more sensitivity to vegetables (18.18%) and cannabis (44.44%) compared to the optical and SAR combinations in Table 5. Amongst the optical and SAR combinations, the optical and VV fusion in trial 5 exhibited the highest sensitivity to vegetables (13.64%), while the optical and VH fusion in trial 4 exhibited the highest sensitivity to cannabis (33.33%). Fusion of optical data with both VV and VH in trial 6 exhibited superior sensitivity to tea (99.98%) compared to Optical and VH (99.88%) in trial 4, Optical and VV (99.84%) in trial 5, and exclusive use of optical data (99.76%) in trial 3. In order to ascertain whether the classification accuracy improvements obtained by combining optical and SAR were real or just chance events, we performed statistical significance tests at α = 0.95. Table 5 shows that combining optical and SAR data produced a statistically significant improvement as compared to using the best of optical data exclusively (*p* = 0.0005). Figure 4 presents the classification maps we obtained from fusing Sentinel-1 and Sentinel-2.
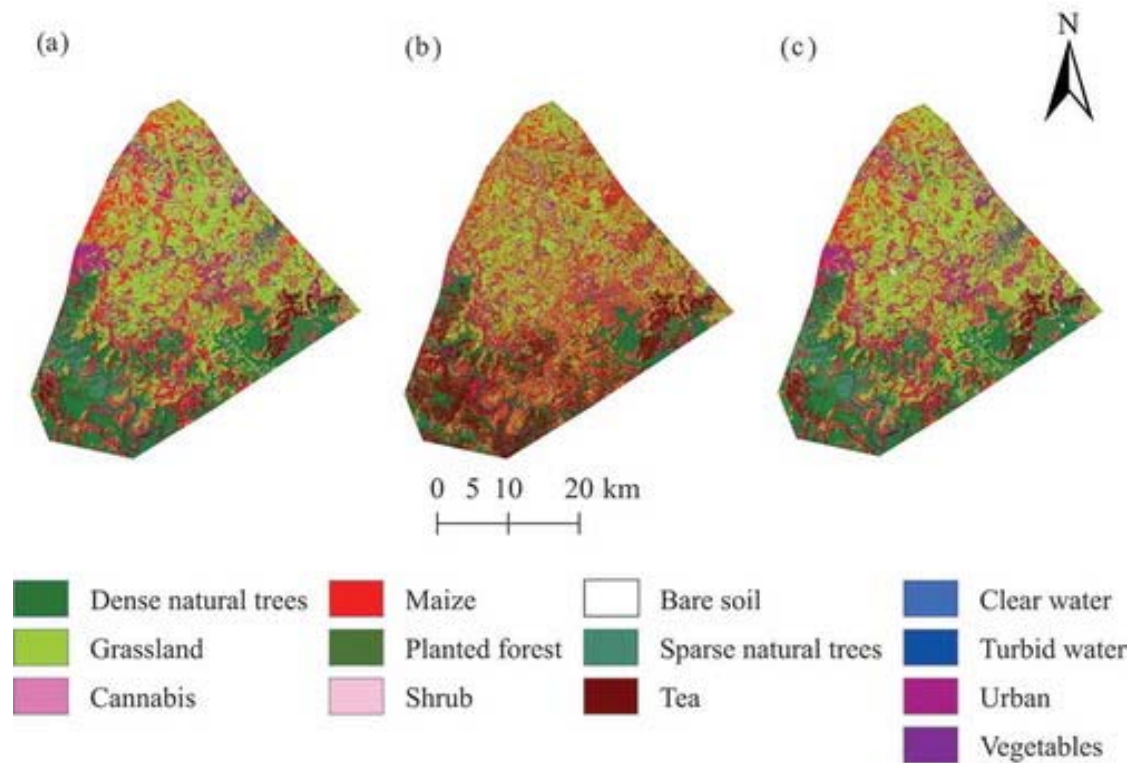
Figure 4. Classification of ORTDM with Sentinel-2 and Sentinel-1 fused: (*a*) Trial 4, (*b*) Trial 5, (*c*) Trial 6.

3.3. Results of model stacking

We investigated model stacking as another technique to improve mapping accuracy. To find the most efficient way to stack the models, we trained Xgboost, RF, SVM, ANN, and NB and then computed a correlation matrix comparing the algorithms. We performed this on the combined Sentinel-2 variables (bands + indices). Table 6 shows how the models correlated.

Table 6. Model correlation matrix.

	Xgboost	RF	SVM	ANN	NB
Xgboost	1.00	0.55	0.49	0.71	0.42
RF	0.55	1.00	0.94	0.73	0.69
SVM	0.49	0.94	1.00	0.58	0.79
ANN	0.71	0.73	0.58	1.00	0.67
NB	0.42	0.69	0.79	0.67	1.00

The levels of correlation between Xgboost and the other algorithms were not too strong (0.55, 0.49, 0.71, and 0.42). RF and SVM correlated strongly (0.94) while SVM and NB also had high correlation (0.79). We observed that Xgboost and ANN (0.71) had high correlation as compared to Xgboost and RF (55), Xgboost and SVM (0.49), Xgboost and NB (0.42). Based on the correlation matrix, we concluded, in the final analysis, that the least correlated models were Xgboost, RF, and NB. We therefore ran two model-stacking trials, one including all the algorithms, and the other one including Xgboost, RF, and NB only. Table 7 is a summary of the model stacking results.

Table 7. Results of model stacking vs. individual models.

Method	OA (%)	K
[a] Xgboost	89.09	75.95
ANN	86.88	81.45
RF	85.03	70.13
SVM	84.92	81.33
NB	84.37	66.34
Model stacking		
[b] Xgboost, RF, SVM, ANN, NB	93.97	88.12
[c] Xgboost, RF, NB	96.06	89.70
c − b = 2.09%, p = 0.0242		
c − a = 6.97%, p = 0.0100		

Amongst the five individual algorithms, Xgboost achieved the highest overall accuracy (89.09%). Stacking the algorithms without ANN and SVM attained higher accuracy (96.06%) than stacking all the algorithms indiscriminately (93.97%). The improvement attained by stacking the models based on correlation tests was statistically significant ($α$ = 0.95, p = 0.0242). Model stacking also produced better results as compared to using a single classifier (statistically significant at $α$ = 0.95, p = 0.0100). Table 8 is a summary of per-class results obtained through model stacking.

Table 8. Detailed results of model stacking compared to single-model classification.

Class	Xgboost		Xgboost, RF, SVM, ANN, NB		Xgboost, RF, NB	
	SE	SP	SE	SP	SE	SP
Maize	100.00	99.98	100.00	99.98	100.00	99.99
Vegetables	9.09	100.00	0.00	100.00	9.09	100.00
Cannabis	22.22	100.00	22.22	100.00	27.71	100.00
Tea	99.76	99.80	99.76	99.90	99.76	99.80
Planted forest	90.00	100.00	91.11	99.93	92.28	99.91
Grassland	87.91	98.63	99.17	89.71	99.35	90.01
Urban	96.86	88.82	79.47	98.34	79.53	98.70
Soil	42.11	99.98	24.67	99.99	43.20	99.98
Clear water	95.00	100.00	95.00	100.00	95.00	100.00
Dense natural trees	88.03	99.90	85.79	99.95	86.62	99.97
Sparse natural trees	86.96	99.64	86.61	99.64	93.15	66.69
Turbid water	100.00	100.00	100.00	100.00	100.00	100.00
Shrubs	8.87	99.94	7.25	99.99	8.87	99.99
OA (%)	89.09		93.97		96.09	
K	75.95		88.12		89.70	

Sensitivity of the stacked models to maize and tea did not change as compared to the exclusive use of Xgboost. However, sensitivity to vegetables decreased to 0.00% with the 5 model ensemble, while remaining at 9.09% with the 3 model ensemble. The 5 model ensemble's sensitivity to cannabis remained at 22.22% while increasing to 27.71% with the 3 model ensemble. The differences in OA between the single-model classification and the ensembles are mainly due to increase in sensitivity and specificity in the non-crop information classes. Figure 5 presents the classification maps obtained from model stacking.
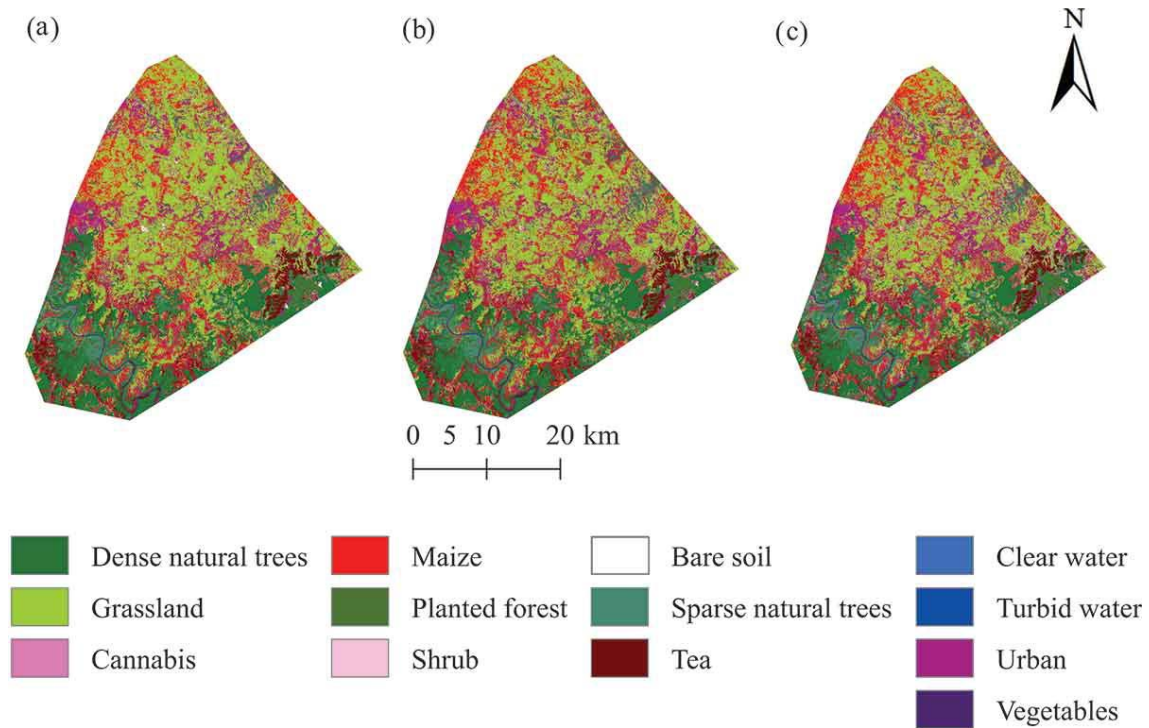
Figure 5. Classification of ORTDM with model stacking: (*a*) Xgboost, (*b*) Xgboost, ANN, RF, SVM, NB, (*c*) Xgboost, RF, NB.

4. Discussion and conclusions

We fused optical and SAR data to map a smallholder agricultural landscape. Among the optical datasets, bands 2, 4, 8A, and 11 proved to be very crucial for discriminating surface features in a heterogeneous agricultural landscape, and were found to be equally effective in similar studies (De Olivier Santos et al. 2019; Zhang et al. 2019). This complementarity highlights the utility of combining NIR, red and red edge bands, which are sensitive to vegetation dynamics, with the SWIR, which highlights urban features. This underscores the importance of including the SWIR band when mapping crop fields that are proximal to urban features. In other studies, the SWIR band has also shown to improve vegetation mapping across urban and heterogeneous landscapes (Hartling et al. 2019; Sidike et al. 2019).

We elected to systematically add SAR data to the optical variables because most studies similar to ours have found the latter to attain higher accuracy than the former (Clerici, Valbuena Calderón, and Posada 2017; Denize et al. 2019; Fontanelli et al. 2014; Mercier et al. 2019; Tavares et al. 2019). Combining optical data with the VH bands improved overall accuracy and sensitivity to tea while reducing sensitivity to vegetables and cannabis. In overall, maize and tea were mapped with very high accuracy. Although most of the maize fields were smaller than 2 ha, maize is the majority class in the training data, while the tea fields are bigger in size. The misclassification of vegetables and cannabis can be attributed to various interacting factors including, the sizes of both cannabis and vegetable fields, most of which ranged between about 0.01 and 1.00 ha. Secondly, there was poor plant spacing and irregular planting patterns particularly in the cannabis fields, and big patches of bare soil in both cannabis and vegetable fields. In this situation, reflectance from crop canopy is hugely affected by background interference from soil, which has its own dynamic spectral properties, resulting in distortion of crop spectral reflectance (Prudnikova et al. 2019). Thirdly, due to the rarity of vegetable farming in the area, the number of training points for vegetables was small compared to the other classes. Imbalanced training data often lead to imbalanced learning, which can pose a challenge to classification (Douzas et al. 2019). Fourthly, the cannabis fields are located in obscure and remote locations because most of the cannabis farming in the area is unlicensed.

In any case, the VH polarized band proved more important than the VV channel. Although some studies report marginal differences between these polarimetric bands (Abdikan et al. 2016; Inglada et al. 2016; Van Tricht et al. 2018; Whelen and Siqueira 2018), the VH band has higher sensitivity to vegetation and other land cover types than the VV band (Ban 2016; Dimov et al. 2017; Rajah, Odindi, and Mutanga 2018). This can be explained by the fact that while VV backscatter is negatively affected by temporal changes in the scattering mechanism (Xu et al. 2019),VH backscatter is a better characterizer of vegetation because it is indicative of volume scattering (Brisco et al. 1992; Vreugdenhil et al. 2018). On the other hand, joint-use of the VH and VV polarimetric bands outperformed single-use of either bands.

We applied model stacking to find the most effective way of combining classifiers and improving classification accuracy. Amongst the base-classifiers, Xgboost achieved higher classification accuracy, outperforming the second best classifier (ANN) by 2.21%. Model correlations between Xgboost and the other classifiers were low to moderate, warranting stacking of Xgboost with any of the four classifiers. However, we observed that SVM and RF (0.94), SVM and NB (0.79) correlations were high. We also observed that Xgboost and ANN correlated strongly as compared to Xgboost and RF, Xgboost and SVM, Xgboost and NB. Model stacking does not add much advantage in cases where base models have strongly correlated predictions. We therefore optimized ensemble modelling by stacking the models analytically. While stacking of all the models increased accuracy from 89.09% to 93.97%, exclusion of ANN and SVM increased classification accuracy from 89.09% to 96.06% (statistically significant at α = 0.95, p = 0.04).

We learned from this study that successful mapping of a fragmented agricultural landscape is a function of objectively derived datasets, adapted to geographic context, and an informed optimization of mapping algorithms. Although both image fusion and model stacking improved classification accuracy, we observed that adding SAR to optical data achieved higher accuracy than merely applying model stacking to optical data. We recommend that future investigations should apply model stacking on fused SAR and optical data for even better results. Since this method produced a very high mapping accuracy of maize, we recommend that it be tested in the calculation of maize crop statistics in smallholder farming areas. The approach is objective and not limited to the study area in the sense that the datasets are adapted to the geographic context through variable ranking, while model stacking is informed by model comparison tests. We recommend that future investigations should consider experimentation with different image fusion techniques, SAR techniques, and different sets of machine learning/deep learning algorithms. We also recommend follow up studies including a wider test trying of the techniques provided in this paper by mapping the distributions of smallholder crop fields in other places. Embracing this recommendation is advisable because it is potentially capable of securitizing crop production by enabling smallholder farmer support from insurers, creditors and the government.

References

Abdikan, S., M. Sanli, M. Ustuner, and F. Calo. 2016. "Land Cover Mapping Using SENTINEL-1 SAR Data." *ISPRS-International Archives of the Photogrammetry, Remote Sensing and Spatial Information Sciences* 757–761. https://doi.org/DOI: 10.5194/isprs-archives-XLI-B7-757-2016

African Smallholder Farmers Group (ASFG). 2013. "Supporting Smallholder Farmers in Africa". *African Smallholder Farmers Group* 71. http://www.asfg.org.uk/framework-report/overview

Aguilar, R., R. Zurita-Milla, E. Izquierdo-Verdiguier, and R. A. de By. 2018. "A Cloud-based Multi-temporal Ensemble Classifier to Map Smallholder Farming Systems." *Remote Sensing* 10 (5): 5. doi:10.3390/rs10050729.

Akpalu, D. 2013. "Agriculture Extension Service Delivery in a Semi-arid Rural Area in South Africa: The Case Study of Thorndale in the Limpopo Province." *African Journal of Food, Agriculture, Nutrition and Development* 13 (4): 8058–8076. doi:org/http://hdl.handle.net.uplib.idm.oclc.org/1807/56061.

Aliber, M., and T. G. B. Hart. 2009. "Should Subsistence Agriculture Be Supported as a Strategy to Address Rural Food Insecurity?" *Agrekon* 48 (4): 434–458. doi:10.1080/03031853.2009.9523835.

Ban, Y. 2016. *Multitemporal Remote Sensing: Methods and Applications*. Springer, Cham, Switzerland. doi:10.1007/978-3-319-47037-5.

Bembridge, T. J. (2000). "Guidelines for Rehabilitation of Small-scale Farmer Irrigation Schemes in South Africa". *Water Research Commission*.. http://www.wrc.org.za/wp-content/uploads/mdocs/891-1-00.pdf

Breiman, L. 2001. "Random Forests." *Machine Learning* 45 (1): 5–32. doi:org/10.1023/A:1010933404324.

Brisco, B., F. T. Ulaby, and R. Protz. 1984. "Improving Crop Classification through Attention to the Timing of Airborne Radar Acquisitions." *Photogrammetric Engineering & Remote Sensing* 50 (6): 739–745.

Brisco, B., R. J. Brown, J. G. Gairns, and B. Snider. 1992. "Temporal Ground-based Scatterometer Observations of Crops in Western Canada." *Canadian Journal of Remote Sensing* 18 (1): 14–21. doi:10.1080/07038992.1992.10855138.

Carletto, C., D. Jolliffe, and R. Banerjee 2013. "The Emperor Has No Data! Agricultural Statistics in Sub-Saharan Africa". *World Bank Working Paper*. http://mortenjerven.com/wp-content/uploads/2013/04/Panel-3-Carletto.pdf

Chapagain, T., and M. N. Raizada. 2017. "Impacts of Natural Disasters on Smallholder Farmers: Gaps and Recommendations." *Agriculture and Food Security* 6 (1): 1–16. doi:10.1186/s40066-017-0116-6.

Chen, T., and C. Guestrin 2016. "XGBoost: A Scalable Tree Boosting System". *Proceedings of the ACM SIGKDD International Conference on Knowledge Discovery and Data Mining*, 13-17-Augu, 785–794, San Francisco, California, USA. doi:10.1145/2939672.2939785.

Clerici, N., C. A. Valbuena Calderón, and J. M. Posada. 2017. "Fusion of Sentinel-1a and sentinel-2A Data for Land Cover Mapping: A Case Study in the Lower Magdalena Region, Colombia." *Journal of Maps* 13 (2): 718–726. doi:10.1080/17445647.2017.1372316.

Cortez, C., and V. Vapnik. 1995. "Support-Vector Networks." *Machine Learning* 20: 273–297. doi:10.1109/64.163674.

De Oliveira Santos, C. L. M., R. A. C. Lamparelli, G. K. Dantas Araújo Figueiredo, S. Dupuy, J. Boury, A. C. Luciano, R. D. Torres, and G. Le Maire. 2019. "Classification of Crops, Pastures, and Tree Plantations along the Season with Multi-sensor Image Time Series in a Subtropical Agricultural Region." *Remote Sensing* 11 (3). doi:doi:10.3390/rs11030334

Debats, S. R., D. Luo, L. D. Estes, T. J. Fuchs, and K. Caylor. 2016. "A Generalized Computer Vision Approach to Mapping Crop Fields in Heterogeneous Agricultural Landscapes." *Remote Sensing of Environment* 179: 210–221. doi:10.1016/j.rse.2016.03.010.

Denize, J., L. Hubert-Moy, J. Betbeder, S. Corgne, J. Baudry, and E. Pottier. 2019. "Evaluation of Using Sentinel-1 and −2 Time-series to Identifywinter Land Use in Agricultural Landscapes." *Remote Sensing* 11: 1. doi:10.3390/rs11010037.

Department of Rural Development and Land Reform (DRDLR). 2016. "*O.r. Tambo District Business Plan*". http://www.ruraldevelopment.gov.za/phocadownload/Agri-parks/Business-Plans/OR-Tambo/or tambo dm final master agri-park business plan section 1.pdf

Devereux, S. 2007. "The Impact of Droughts and Floods on Food Security and Policy Options to Alleviate Negative Effects." *Agricultural Economics* 37 (S1): 47–58. doi:10.1111/j.1574-0862.2007.00234.x.

Dhumal, R., Y. Rajendra, K. V. Kale, and S. C. Mehrotra. 2013. "Classification of Crops from Remotely Sensed Images Using Fuzzy Classification Approach." *International Journal of Advanced Research in Computer Science and Software Engineering* 3 (7): 758–761.

Dimov, D., F. Low, M. Ibrakhimov, G. Stulina, and C. Conrad 2017. "SAR and Optical Time Series for Crop Classification". *International Geoscience and Remote Sensing Symposium (IGARSS)*, 2017-July(July), 811–814, Fort Worth, Texas, USA. doi:10.1109/IGARSS.2017.8127076.

Douzas, G., F. Bacao, J. Fonseca, and M. Khudinyan. 2019. "Imbalanced Learning in Land Cover Classification: Improving Minority Classes' Prediction Accuracy Using the Geometric SMOTE Algorithm." *Remote Sensing* 11 (24): 24. doi:10.3390/rs11243040.

Džeroski, S., and B. Ženko. 2004. "Is Combining Classifiers with Stacking Better than Selecting the Best One?" *Machine Learning* 54 (3): 255–273. doi:10.1023/B:MACH.0000015881.36452.6e.

Eastern Cape Socio Economic Consultative Council (ECSECC). 2014. "Socio-Economic Profile of Eastern Cape Province". http://www.ecsecc.org

Eugster, M. J. A., T. Hothorn, and F. Leisch 2008. "Exploratory and Inferential Analysis of Benchmark Experiments". *Ludwigs-Maximilians-Universitat Munchen, Department of Statistics, Technical Report, Number 030*, (030).

Fanadzo, M., and B. Ncube. 2018. "Challenges and Opportunities for Revitalising Smallholder Irrigation Schemes in South Africa." *Water SA* 44 (3): 436–447. doi:10.4314/wsa.v44i3.11.

FAO. 2016. "Crop Yield Forecasting: Methodological and Institutional Aspects". https://gsars.org/en/crop-yield-forecasting-methodological-and-institutional-aspects/

Fontanelli, G., A. Crema, R. Azar, D. Stroppiana, P. Villa, and M. Boschetti. 2014. "Agricultural Crop Mapping Using Optical and SAR Multi-temporal Seasonal Data: A Case Study in Lombardy Region, Italy." *International Geoscience and Remote Sensing Symposium (IGARSS)*, no. July: 1489–1492. doi:10.1109/IGARSS.2014.6946719.

Forkuor, G., C. Conrad, M. Thiel, T. Ullmann, and E. Zoungrana. 2014. "Integration of Optical and Synthetic Aperture Radar Imagery for Improving Crop Mapping in Northwestern Benin, West Africa." *Remote Sensing* 6 (7): 6472–6499. doi:10.3390/rs6076472.

Géron, A. 2019. *Hands-On Machine Learning with Scikit-Learn and TensorFlow*. O'Reilly Media, Sebastopol, California, USA.

Graeub, B. E., M. J. Chappell, H. Wittman, S. Ledermann, R. B. Kerr, and B. Gemmill-Herren. 2016. "The State of Family Farms in the World." *World Development* 87: 1–15. doi:10.1016/j.worlddev.2015.05.012.

Hartling, S., V. Sagan, P. Sidike, M. Maimaitijiang, and J. Carron. 2019. "Urban Tree Species Classification Using a Worldview-2/3 and liDAR Data Fusion Approach and Deep Learning." *Sensors (Switzerland)* 19 (6): 1–23. doi:10.3390/s19061284.

Harvey, C. A., M. Saborio-Rodríguez, M. R. Martinez-Rodríguez, B. Viguera, A. Chain-Guadarrama, R. Vignola, and F. Alpizar. 2018. "Climate Change Impacts and Adaptation among Smallholder Farmers in Central America." *Agriculture and Food Security* 7 (1): 1–20. doi:10.1186/s40066-018-0209-x.

Hatfield, J. L., and J. H. Prueger. 2010. "Value of Using Different Vegetative Indices to Quantify Agricultural Crop Characteristics at Different Growth Stages under Varying Management Practices." *Remote Sensing* 2 (2): 562–578. doi:10.3390/rs2020562.

Hothorn, T., F. Leisch, A. Zeileis, and K. Hornik. 2005. "The Design and Analysis of Benchmark Experiments." *Journal of Computational and Graphical Statistics* 14 (3): 675–699. doi:10.1198/106186005X59630.

Hur, J. H., S. Y. Ihm, and Y. H. Park. 2017. "A Variable Impacts Measurement in Random Forest for Mobile Cloud Computing." *Wireless Communications and Mobile Computing* 2017. doi:10.1155/2017/6817627.

Inglada, J., A. Vincent, M. Arias, and C. Marais-Sicre. 2016. "Improved Early Crop Type Identification by Joint Use of High Temporal Resolution Sar and Optical Image Time Series." *Remote Sensing* 8 (5): 5. doi:10.3390/rs8050362.

Iortyom, E. T., S. P. Mazinyo, and W. Nel. 2018. "Analysis of the Economic Impact of Rural Enterprise Development Hub Project on Maize Farmers in Mqanduli, South Africa." *Indian Journal of Agricultural Research* 52 (3): 243–249. doi:10.18805/IJARe.A-319.

Jiang, Z., A. R. Huete, K. Didan, and T. Miura. 2008. "Development of a Two-band Enhanced Vegetation Index without a Blue Band." *Remote Sensing of Environment* 112 (10): 3833–3845. doi:10.1016/j.rse.2008.06.006.

Jordaan, A., D. Makate, T. Mashego, M. Ligthelm, J. Malherbe, B. Mwaka, … V. Zyl 2017. "Vulnerability, Adaptation to and Coping with Drought: The Case of Commercial and Subsistence Rain Fed Farming in the Eastern Cape. In *Volume II*". www.wrc.org.za%0AThe

Keita, N., E. Carfagna, and G. Mu'Ammar 2010. "Issues and Guidelines for the Emerging Use of GPS and PDAs in Agricultural Statistics in Developing Countries". *The Fifth International Conference on on Agricultural Statistics (ICAS V)*, 12–15, Kampala, Uganda. http://www.fao.org/fileadmin/templates/ess/documents/meetings_and_workshops/ICAS5/PDF/ICASV _2.2_097_Paper_Keita.pdf

Khapayi, M., and P. R. Celliers. 2016. "Factors Limiting and Preventing Emerging Farmers to Progress to Commercial Agricultural Farming in the King William's Town Area of the Eastern Cape Province, South Africa." *South African Journal of Agricultural Extension* 44 (1): 1–10. doi:10.17159/2413-3221/2016/v44n1a374.

Lowder, S. K., J. Skoet, and T. Raney. 2016. "The Number, Size, and Distribution of Farms, Smallholder Farms, and Family Farms Worldwide." *World Development* 87: 16–29. doi:10.1016/j.worlddev.2015.10.041.

Manderson, A., N. Kubayi, and S. Drimie 2016. "SAFL-Drought-Impact-Assessment-2016-Final". *Southern Africa Food Lab*, (FEBRUARY). http://www.southernafricafoodlab.org/wp-content/uploads/2016/06/SAFL-Drough-Impact-Assessment-2016-Final.pdf

Mercier, A., J. Betbeder, F. Rumiano, J. Baudry, V. Gond, L. Blanc, … L. Hubert-Moy. 2019. "Evaluation of Sentinel-1 and 2 Time Series for Land Cover Classification of Forest–Agriculture Mosaics in Temperate and Tropical Landscapes." *Remote Sensing* 11 (8): 1–20. doi:10.3390/rs11080979.

Merz, C. J. 1999. "Using Correspondence Analysis to Combine Classifiers." *Machine Learning* 36 (1): 33–58. doi:10.1023/A:1007559205422.

Mugambiwa, S. S., and H. M. Tirivangasi. 2017. "Climate Change: A Threat Towards Achieving "Sustainable Development Goal Number Two" (End Hunger, Achieve Food Security and Improved Nutrition and Promote Sustainable Agriculture) in South Africa." *Jamba: Journal of Disaster Risk Studies* 9 (1): 1–6. doi:10.4102/jamba.v9i1.350.

Municipality, O. R. T. D. 2017. "Annual Report 2016/2017". In *O.R. Tambo District Municipality* (Vol. 20). doi:10.20622/jltajournal.20.0_0.

Nielsen, D. 2016. "Tree Boosting with XGBoost". *Master's Thesis, Norwegian University of Science and Technology*, (December), 2016. doi:10.1111/j.1758-5899.2011.00096.x.

Nieuwoudt, L., and J. Groenewald. 2003. *The Challenge of Change: Agriculture, Land and the South African Economy*. Pietermaritzburg: University of KwaZulu-Natal Press.

Persello, C., V. A. Tolpekin, J. R. Bergado, and R. A. de By. 2019. "Delineation of Agricultural Fields in Smallholder Farms from Satellite Images Using Fully Convolutional Networks and Combinatorial Grouping." *Remote Sensing of Environment* 231 (April). doi:10.1016/j.rse.2019.111253.

Phadikar, S., and J. Goswami 2016. "Vegetation Indices Based Segmentation for Automatic Classification of Brown Spot and Blast Diseases of Rice". *2016 3rd International Conference on Recent Advances in Information Technology, RAIT 2016*, 284–289, Dhanbad, India. https://doi.org/10.1109/RAIT.2016.7507917

Prudnikova, E., I. Savin, G. Vindeker, P. Grubina, E. Shishkonakova, and D. Sharychev. 2019. "Influence of Soil Background on Spectral Reflectance of Winter Wheat Crop Canopy." *Remote Sensing* 11 (16): 16. doi:10.3390/rs11161932.

Rajah, P., J. Odindi, and O. Mutanga. 2018. "Feature Level Image Fusion of Optical Imagery and Synthetic Aperture Radar (SAR) for Invasive Alien Plant Species Detection and Mapping." *Remote Sensing Applications: Society and Environment* 10: 198–208. doi:10.1016/j.rsase.2018.04.007.

Rao, N. R. 2008. "Development of a Crop-specific Spectral Library and Discrimination of Various Agricultural Crop Varieties Using Hyperspectral Imagery." *International Journal of Remote Sensing* 29 (1): 131–144. doi:10.1080/01431160701241779.

Rapsomanikis, G. 2015. "The Economic Lives of Smallholder Farmers." *Fao* 39. doi:10.5296/rae.v6i4.6320.

Ripley, B. D. 1996. "Pattern Recognition and Neural Networks". *Cambridge University Press*. doi:org/10.1017/CBO9780511812651.

Rwanga, S. S., and J. M. Ndambuki. 2017. "Accuracy Assessment of Land Use/Land Cover Classification Using Remote Sensing and GIS." *International Journal of Geosciences* 08 (4): 611–622. doi:10.4236/ijg.2017.84033.

Salas, E. A. L., S. K. Subburayalu, B. Slater, K. Zhao, B. Bhattacharya, R. Tripathy, … P. Parekh. 2019. "Mapping Crop Types in Fragmented Arable Landscapes Using AVIRIS-NG Imagery and Limited Field Data." *International Journal of Image and Data Fusion* 11 (1): 33–56. doi:10.1080/19479832.2019.1706646.

Samberg, L. H., J. S. Gerber, N. Ramankutty, M. Herrero, and P. C. West. 2016. "Subnational Distribution of Average Farm Size and Smallholder Contributions to Global Food Production." *Environmental Research Letters* 11 (12): 12. doi:10.1088/1748-9326/11/12/124010.

Sidike, P., V. Sagan, M. Maimaitijiang, M. Maimaitiyiming, N. Shakoor, J. Burken, … F. B. Fritschi. 2019. "dPEN: Deep Progressively Expanded Network for Mapping Heterogeneous Agricultural Landscape Using WorldView-3 Satellite Imagery." *Remote Sensing of Environment* 221 (April2018): 756–772. doi:10.1016/j.rse.2018.11.031.

Solares, C., and A. Sanz 2007. "Bayesian Networks in the Classification of Multispectral and Hyperspectral Remote Sensing Images". *3rd WSEAS International Conference on Remote Sensing*, (June), 83–86, Venice, Italy.
http://www.researchgate.net/publication/228952757_Bayesian_Networks_in_the_Classification_of_M ultispectral_and_Hyperspectral_Remote_Sensing_Images/file/9c96051cc21264fed2.pdf

Sonobe, R., Y. Yamaya, H. Tani, X. Wang, N. Kobayashi, and K. Mochizuki. 2018. "Crop Classification from Sentinel-2-derived Vegetation Indices Using Ensemble Learning." *Journal of Applied Remote Sensing* 12 (2): 1. doi:10.1117/1.jrs.12.026019.

Souri, A. H., and S. Vajedian. 2015. "Dust Storm Detection Using Random Forests and Physical-based Approaches over the Middle East." *Journal of Earth System Science* 124 (5): 1127–1141. doi:10.1007/s12040-015-0585-6.

Tavares, P. A., N. E. S. Beltrão, U. S. Guimarães, and A. C. Teodoro. 2019. "Integration of Sentinel-1 and Sentinel-2 for Classification and LULC Mapping in the Urban Area of Belém, Eastern Brazilian Amazon." *Sensors (Switzerland)* 19: 5. doi:10.3390/s19051140.

UNCTAD. 2015. "The Role of Smallholder Farmers in Sustainable Commodities Production and Trade". *United Nations Conference on Trade and Development, 12875* (July), Geneva, Switzerland.

Useya, J., and S. Chen. 2018. "Comparative Performance Evaluation of Pixel-Level and Decision-Level Data Fusion of Landsat 8 OLI, Landsat 7 ETM+ and Sentinel-2 MSI for Crop Ensemble Classification." *IEEE Journal of Selected Topics in Applied Earth Observations and Remote Sensing* 11 (11): 4441–4451. doi:10.1109/JSTARS.2018.2870650.

Useya, J., and S. Chen. 2019. "Exploring the Potential of Mapping Cropping Patterns on Smallholder Scale Croplands Using Sentinel-1 SAR Data." *Chinese Geographical Science* 29 (4): 626–639. doi:10.1007/s11769-019-1060-0.

Van Tricht, K., A. Gobin, S. Gilliams, and I. Piccard. 2018. "Synergistic Use of Radar Sentinel-1 and Optical Sentinel-2 Imagery for Crop Mapping: A Case Study for Belgium." *Remote Sensing* 10 (10): 1–22. doi:10.3390/rs10101642.

Von Fintel, D., and L. Pienaar. 2016. "Small-Scale Farming and Food Security: The Enabling Role of Cash Transfers in South Africa's Former Homelands." *IZA Discussion Paper* 10377 (November). doi:10.22004/ag.econ.211916.

Vreugdenhil, M., W. Wagner, B. Bauer-Marschallinger, I. Pfeil, I. Teubner, C. Rüdiger, and P. Strauss. 2018. "Sensitivity of Sentinel-1 Backscatter to Vegetation Dynamics: An Austrian Case Study." *Remote Sensing* 10 (9): 1–19. doi:10.3390/rs10091396.

Whelen, T., and P. Siqueira. 2018. "Time-series Classification of Sentinel-1 Agricultural Data over North Dakota." *Remote Sensing Letters* 9 (5): 411–420. doi:10.1080/2150704X.2018.1430393.

Wolpert, D. 1992. "Stacked Generalization (Stacking)." *Neural Networks* 5 (2): 241–259. doi:10.1016/S0893-6080(05)80023-1.

Wu, Q., L. Wang, and J. Wu. 2012. "Ensemble Learning on Hyperspectral Remote Sensing Image Classification." *Advanced Materials Research* 546–547: 508–513. doi:10.4028/www.scientific.net/AMR.546-547.508.

Xu, L., H. Zhang, C. Wang, B. Zhang, and M. Liu. 2019. "Crop Classification Based on Temporal Information Using Sentinel-1 SAR Time-series Data." *Remote Sensing* 11 (1): 1–18. doi:10.3390/rs11010053.

Xue, J., and B. Su. 2017. "Significant Remote Sensing Vegetation Indices: A Review of Developments and Applications." *Journal of Sensors* 2017: 1–17. doi:10.1155/2017/1353691.

Zha, Y., J. Gao, and S. Ni. 2003. "Use of Normalized Difference Built-up Index in Automatically Mapping Urban Areas from TM Imagery." *International Journal of Remote Sensing* 24 (3): 583–594. doi:10.1080/01431160304987.

Zhang, T. X., J. Y. Su, C. J. Liu, and W. H. Chen. 2019. "Potential Bands of Sentinel-2A Satellite for Classification Problems in Precision Agriculture." *International Journal of Automation and Computing* 16 (1): 16–26. doi:10.1007/s11633-018-1143-x.

Zhou, T., J. Pan, P. Zhang, S. Wei, and T. Han. 2017. "Mapping Winter Wheat with Multi-temporal SAR and Optical Images in an Urban Agricultural Region." *Sensors (Switzerland)* 17 (6): 1–16. doi:10.3390/s17061210.

Zurita-Milla, R., E. Izquierdo-Verdiguier, and R. A. De By 2017. "Identifying Crops in Smallholder Farms Using Time Series of WorldView-2 Images". *2017 9th International Workshop on the Analysis of Multitemporal Remote Sensing Images, MultiTemp 2017*, 17–19. https://doi.org/10.1109/Multi-Temp.2017.8035246